

### 5.3 Flow over an obstacle.

We now consider the Froude number plane representation of solutions for flow over topography in a channel of constant width. Continuing to follow Armi (1986), it is helpful to rewrite the energy equation (5.2.13) in the normalized form

$$\frac{1}{2}F_1^{4/3} - \frac{1}{2}Q_r^{-2/3}F_2^{4/3} + F_1^{-2/3} = \frac{g'z_r^* - \Delta B^*}{(g'Q_1^*/w^*)^{2/3}} \quad (5.3.1)$$

One interpretation of the quantity on the right-hand side follows by imagining that the straight channel is connected to an infinitely wide, quiescent basin as described above. Use of (5.2.10) and (5.2.11) then leads to

$$\frac{g'z_r^* - \Delta B^*}{(g'Q_1^*/w^*)^{2/3}} = \frac{g'd_{1\infty}^*}{(g'Q_1^*/w^*)^{2/3}} = d_{1\infty}$$

The parameter  $d_{1\infty}$  is the dimensionless upper layer thickness in the hypothetical wide basin. It may also be regarded as a measure of the potential energy in the basin, smaller  $d_{1\infty}$  being associated with higher interface values and therefore higher potential energy.

In some applications the transport ratio  $Q_r$  may be regarded as fixed. For example, some ocean straits are constrained to carry a net volume flux that is close to zero, so that  $Q_r$  has a value close to -1. Let us then assume that  $Q_r$  is constant. Then there is a family of solutions to (5.3.1), each member having a particular upstream state as indicated by the value of  $d_{1\infty}$ . These solutions can be represented as a family of curves plotted in the Froude number plane (e.g. Figure 5.3.1a). The case shown has  $|Q_r| = 1$  and the  $d_{1\infty} = \text{constant}$  solutions are represented by the thicker curves. In the absence of hydraulic jumps or of other sources of dissipation, a solution must follow one of these curves. Some of these curves intersect the critical flow diagonal, raising the possibility that corresponding solutions can be critically controlled. Froude number diagrams for other values of  $Q_r$  have similar qualitative aspects (Armi, 1986) and we can therefore discuss most of the general features of the solutions using the one figure. Note that  $Q_r$  and  $Q_1^*$  enter (5.3.1) to  $2/3$  powers and therefore a solution curve valid for a combination  $(Q_r, Q_1^*)$  is also valid for  $(-Q_r, Q_1^*)$ ,  $(Q_r, -Q_1^*)$ , or  $(-Q_r, -Q_1^*)$ . The direction of flow in a given layer for a particular solution is therefore arbitrary. Each curve yields four possible solutions corresponding to different directions of flow in the two layers. However, not all possibilities may be realizable: the stability of the flow and its ability to form hydraulic jumps does depend on the direction of layer transport. An obvious example is a unidirectional flow that is stable according to (5.2.2) but becomes unstable due to the increased interfacial shear that is created when the direction of flow in one of the layers is reversed. More subtle examples arise when a change in direction of a layer flux gives rise to the shock-forming instability (Figure 1.4.4).

Now suppose that the value of  $d_{1\infty}$  is given along with the topographic function  $h^*(y^*)$ . In order to construct a solution one needs to know how to move along the appropriate curve of constant  $d_{1\infty}$  as  $h^*$  varies. This link between the solution and the topography is provided by (5.2.14), which can be cast in terms of the Froude numbers as

$$Q_r^{2/3} F_1^{-2/3} + F_2^{-2/3} = q_2^{-2/3}, \quad (5.3.2)$$

where

$$q_2 = \frac{Q_2^*}{[z_T^* - h^*(y^*)]^{3/2} g'^{1/2} w^*}.$$

The thin contours drawn in Figure 5.3.1a are ones of constant  $q_2$ . Since  $Q_2^*$ ,  $g'$ , and  $w^*$  remain fixed for a particular steady solution, changes in  $q_2$  with  $y^*$  are entirely due to changes in  $h^*$ . Increases in  $h^*$  lead to increases in  $q_2$  and inspection of Fig. 5.3.1a shows that higher  $h^*$  are generally found by moving away from the origin.

*a. Flow from a deep basin.*

One important class of solutions describes flow originating from an infinitely deep upstream basin that has the same width as the channel. Note that at least one of the layer depths must be infinite (and the corresponding velocity zero) in the basin and therefore the solution curve must begin along the horizontal ( $F_2^2=0$ ) or vertical ( $F_1^2=0$ ) axis (Figure 5.3.1a). Inspection of the figure shows that the only possibilities originate from the horizontal axis. These solutions have  $F_2=0$  in the basin, meaning that the lower layer is infinitely deep and (therefore) stagnant. The reverse situation, a stagnant upstream upper layer with a moving lower layer, is not possible. This asymmetry between the behavior of the upper and lower layers is due to the fact that the topography contacts only the lower layer. Although the formal solutions allow the direction of flow within each layer to be arbitrary, let us assume that the lower layer flow is out of the deep basin. The upper layer flow may then be in either direction, unless otherwise noted. And, we will continue to refer to the latter as the upstream basin, even though the upper layer may flow into it.

Now suppose that the value of  $d_{1\infty}$  is known to be 1.7, so that the solution must lie along the thick curve with that value. Keep in mind that  $d_{1\infty}$  is not the actual upper layer depth in the deep basin, but rather the upper layer depth in a hypothetical reservoir that has infinite width and is therefore quiescent. (This reservoir might be imagined to lie upstream of the deep basin.) The flow state in the deep basin lies where the  $d_{1\infty}=1.7$  curve intersects the  $F_1^2$  axis and is clearly subcritical. An observer moving from the basin into the channel will see an increase in  $h$  and must therefore move upwards along the '1.7' curve to higher contour values of  $q_2$ . If the sill is reached before the critical diagonal is encountered then the solution at points downstream is found by retracing the '1.7' curve back to the  $F_1^2$  axis. In this way a completely subcritical solution is obtained.

The value of  $F_1^2$  is minimal at the sill, meaning that the upper layer depth reaches a maximum (see 5.2.12a). Figure 5.3.1b shows this situation schematically, with the ‘1.7’ solution curve traced over a circuit  $aba$  and the corresponding subcritical solution (inset) experiencing an interfacial dip over the obstacle.

If the sill height is increased to the point where the sill is encountered at the crossing with the critical diagonal, then a transition to supercritical flow is possible. Note that the thick and thin contours make grazing contact with each other along the diagonal, a property that has two important implications. First, the value of the topographic parameter  $q_2$  at that point is the maximum that occurs along the thick curve. That is, the topographic elevation is the highest that can be achieved along that solution curve. The second implication is that the solution may be followed beyond the sill either by continuing upward along the ‘1.7’ curve into the supercritical region or by retracing downward into the subcritical region. This same dilemma arises in the treatment of single-layer flows and it can be shown by similar arguments (see Exercise 3 of the previous section) that the correct option is to continue into supercritical space. The circuit is something like  $abcd$  in Figure 5.3.1b and the interface profile resembles the free surface profile for a hydraulically controlled, single-layer flow (second inset). It is natural to ask what would happen if the sill height is increased even further and we will return to this point shortly.

#### *b. Internal hydraulic jumps.*

Given the similarity with the single-layer case, one might expect a hydraulic jump to arise in the supercritical part of the flow. The problem of shock joining in two layers is more difficult than for the single-layer case due to several factors. First, a transfer of horizontal momentum between the two layers can occur as the result of pressure forces on the steeply sloping interface within a jump. These forces exist in the region where nonhydrostatic effects are expected to be greatest, making a calculation of the pressure force problematic. The difficulty is avoided in single layers due to the fact that the pressure is essentially zero at the free surface. Second, entrainment of one layer into the other or creation of masses of intermediate density can occur as the result of mixing. These transformations complicate the mass, and perhaps the momentum balances. In some cases interfacial instability and mixing occur broadly and cause the transition from supercritical to subcritical flow to occur without any roller or other abrupt feature. An example of this limiting case is shown in the top frame of Figure 1.6.5.

One situation that allows simplification occurs when the two fluids are immiscible, so that  $Q_1^*$  and  $Q_2^*$  are conserved across the jump. This does not occur in nature, but can be simulated as an alternative realization in a laboratory setting. If the jump occurs over a small interval in  $y^*$ , so that  $h^*$  is the same on either side, then the conjugate states must lie along the same constant- $q_2$  curve. As an example, suppose that a hydraulic jump occurs at point  $d$  in Figure 5.3.1b. The jump must return the supercritical flow to a subcritical state and must do so along the thin curve passing through  $d$ . It must therefore connect with another constant energy curve, perhaps at point  $e$ . Determination

of the correct energy curve is quite difficult, however. The jump should cause an overall loss of total energy and it is not obvious what this means for  $\Delta B$ , the difference between the upper and lower layer Bernoulli functions<sup>1</sup>. There have been a number of attempts to come to grips with these problems and the reader is referred to Jiang and Smith (2001a,b), Holland et al. (2002), and references contained therein for more information.

*c. Maximal and submaximal exchange.*

We now rejoin the discussion of the hydraulically controlled solution *abcd* (or a jump-containing variant like *abcde*) and ask what happens if the maximum value of  $q_2$  is increased. This increase could occur as a result of raising the sill or of increasing the value of  $Q_2^*$ , both with the  $d_{1\infty}^*$  fixed. Since the new  $q_2$  is higher than the maximum value possible along the  $d_{1\infty}=1.7$  curve, a time-dependent adjustment of the values of  $d_{1\infty}$  and/or  $Q_r$  must occur. The adjustment involves the generation of a disturbance that propagates upstream and alters the conditions in the deep basin. If the adjustment leaves  $Q_r$  unchanged<sup>2</sup>, the new sill flow is found by following the critical diagonal from point *c* in Figure 5.3.1b down and to the right until the thin curve with the new value of  $q_2$  is encountered. The solution now lies along the (thick) solution curve that intersects this point, and it can be seen that the corresponding  $d_{1\infty}$  is lower than before. In cases where  $Q_r$  is altered, one would have to predict the new value and then consult the Froude number plane diagram appropriate for that value. Determination of the  $Q_r$  generally requires analysis of the upstream disturbance. For purposes of illustration, we will proceed on the assumption that  $Q_r$  remains fixed.

The new solution curve intersects the lower axis at larger values of  $F_1^2$  than before and thus the composite Froude number  $G^2$  of the upstream flow is greater. The upper layer in the basin now has a higher velocity and smaller thickness. As the sill height is increased, one moves to solutions with lower values of  $d_{1\infty}$  and with larger values of  $F_1$  in the basin. Eventually the value  $d_{1\infty}=1.5$  is reached and it can be seen that the corresponding energy curve has an intersection with the  $F_1^2$ -axis at  $F_1^2=1$ . The flow in the basin is now critical. Since the basin is infinitely deep, the lower layer remains at rest and the upper layer moves at speed  $(g'd_1^*)^{1/2}$ . The value of  $G^2$  is unity both in the basin (point *g* in Figure 5.3.1b) and at the sill (point *h*). The intervening flow is subcritical and the flow downstream of the sill is supercritical, perhaps with a hydraulic jump. The situation is represented by the solution *ghi* sketched in the inset.

To this point we have not distinguished between cases of unidirectional flow ( $Q_r=1$ ) and exchange flow ( $Q_r=-1$ ). The solutions discussed can take either form. However, when the flow in the upstream basin becomes critical, important differences arise in how the two situations should be interpreted. We will concentrate on the case of

---

<sup>1</sup> The simplest approach [suggested by Armi (1986)] is to assume that the energy loss in the jump is negligible, so that the conjugate states lie on the same energy curve.

<sup>2</sup> Cases where  $Q_r$  remains fixed can occur in systems with a closed upstream basin with a specified source of volume, often zero. The adjustment to a change in sill height then involves the original upstream disturbance, plus a set of reflected and re-reflected disturbances that pass information about the closed nature of the basin back into the strait.

exchange and revisit unidirectional flow in Part *f* of this section. The upper layer now moves from the strait into the ‘upstream’ basin, right-to-left in the figures, and flows at the critical speed in the basin. A uniform critical flow of this type is typically vulnerable to frictional and dispersive effects and would be difficult to establish in the laboratory. However, a more robust version of the solution can be set up with a slight modification in the geometry of the deep basin. Suppose that the basin is made somewhat wider than the straight section of channel over which the topographic changes occur. Thus the upper layer enters the channel from the ‘downstream’ basin, passes the sill, and enters a subcritical stretch of flow over which the bottom drops away and lower layer deepens. The upper layer accelerates to the critical speed and then exits into the ‘upstream’ basin, which is now wider. Since this layer has become effectively disengaged with the (motionless) lower, it behaves like a single layer and follows the behavior outlined in Chapter 1. In particular, the upper layer becomes supercritical after it exits into the wider basin. The supercritical flow generally terminates in a hydraulic jump. The critical section (point *g*) in the figure is now known as an *exit control*. Propagation of information from the basin into the channel is blocked by this control and by the region of supercritical flow.

The solution with both a sill control and an exit control has been obtained by allowing the value of  $d_{1\infty} = \frac{d_{1\infty}^*}{(g'Q_1^*/w^*)^{2/3}}$  to decrease until the upper layer in the basin becomes critical. It can be shown (Exercise 6) that the corresponding  $d_{1\infty}^*$  is approximately half the fluid depth over the sill. Since  $d_{1\infty}^*$  is a measure of the internal energy of the flow, the decrease in  $d_{1\infty}$  can be accomplished by holding the energy constant and increasing  $|Q_1^*|$ . The threshold state  $d_{1\infty}=1.5$  may therefore be regarded as having the maximum possible upper layer transport for the given available internal energy. As Figure 5.3.1a shows, this value cannot be exceeded by any solution that connects smoothly to a deep upstream basin. There are solutions with larger  $|Q_1^*|$  (i.e., the ones with  $d_{1\infty}>1.5$ ) but none intersect the lower axis.

For flows with only a sill control ( $d_{1\infty}>1.5$ ) the upper layer remains relatively inactive and the behavior of the lower layer is similar to that of a single layer. For example, it can be shown that the layer Froude numbers at the sill fall in the ranges  $0.8 < F_2^2 < 1$  and  $F_1^2 < 0.2$ . Thus the lower layer Froude number is close to the critical value (=1) for a single layer whereas the upper layer Froude number is well into the subcritical range of a single layer. The wave arrested at the sill is dynamically similar to a wave propagating in an environment in which the upper layer is inactive. In contrast, the solution for  $d_{1\infty}=1.5$  involves the engagement of both layers. The exit control takes place where the lower layer is inactive and the sill control takes place where the upper layer is relatively inactive.

For exchange flows it is common to refer to the solution with both a sill control and an approach control as being *maximal*. It has the largest  $|Q_1^*|$ , and therefore the largest exchange transport  $|Q_1^* - Q_2^*|$ , of all the solutions that can be smoothly

connected to a deep basin. The maximization assumes that  $Q_r$  remains fixed. Maximal flow is distinguished by the property that information is allowed to enter the strait from neither the upstream nor the downstream basin. Exchange solutions with just sill controls ( $d_{1\infty} > 1.5$ ) are called *submaximal*. Such flows block downstream information from entering the upstream basin, but not vice versa.

*d. Basins with finite depth.*

For an upstream basin of finite depth there exists a similar family of sill-controlled solutions, each having a single control at the sill, and a limiting solution with two controls. The previously considered solution curves with constant  $d_{1\infty}$  are still in play, but the possible upstream states now lie at finite  $F_2$  and not along the abscissa of the Froude number plane. Suppose that  $d_{1\infty} = 1.7$ , so that the solution lies along the previously considered thick curve in Figure 5.3.1b. Then a solution with a sill control corresponds to something like *bcd*. What makes cases like this more difficult is the exercise of fixing the parameter  $d_{1\infty}$  and identifying the upstream state *b* on the Froude number plane. Even if the transport ratio  $Q_r$ , the channel width  $w^*$ , the basin depth  $z_T^*$  and the sill depth  $D_s = z_T^* - h_m^*$  are known, and  $g'$  and  $d_{1\infty}^*$  are measured, an algebraic process is still required to locate the solution on the Froude number plane. This problem is explored further in the exercises.

Notwithstanding this technical issue, one may proceed by decreasing the value of  $d_{1\infty}$  as before and browsing through the continuum of solutions with sill controls. A limiting solution with two controls will eventually be obtained, this time with  $d_{1\infty} < 1.5$ . The limiting process can be implemented by fixing the topography and the value of  $d_{1\infty}^*$  and increasing the layer fluxes. An example of the limiting case is shown by the curve segment *klmn* in Figure 5.3.1b. The upstream flow in the uniform, finite-depth section of channel (*k* in the figure) is critical. Once the bottom begins to shoal, the flow becomes subcritical (*l*). It then passes through a sill control (*m*) and becomes supercritical (*n*). A profile of the solution is sketched in the inset. For exchange flow, the flux is again maximal over all solutions with the same topography and same  $Q_r$ .

The limiting solution curve that determines the maximal solution for a given finite upstream depth is not easy to locate. However the curve and its  $d_{1\infty}$  value can be calculated and shown to depend on the ratio of the sill depth  $D_s$  to the upstream depth  $z_T^*$ . By applying the definition of  $q_2$  at the upper left intersection of the energy curve with the critical diagonal (i.e. at the sill control) it follows that

$$|Q_2^*| = q_2(D_s / z_T^*) g'^{1/2} w^* D_s^{3/2}. \quad (5.3.3)$$

The function  $q_2(D_s/z_T^*)$  is simply  $q_2$  at the upper left intersection point and the calculation of its dependence on  $D_s/z_T^*$  is described in Exercise 5. For the case of an infinitely deep upstream basin ( $D_s / z_T^* \rightarrow 0$ ),  $q_2$  is given by 0.208, whereas  $q_2 = 0.25$  for the point

labeled  $o$ . Thus the range of variation is quite narrow. As  $D_s / z_T^*$  increases so does the associated  $q_2$  and thus the maximal flux for fixed  $D_s$  and  $g'$  increases as the upstream depth decreases.

Although (5.3.3) bears similarity to the single-layer weir formula (1.4.12), it is more constrained. It is no longer necessary to have knowledge of an upstream interface elevation or the like; the only state variable that needs to be measured is the reduced gravity  $g'$ . The insensitivity of the flux to upstream conditions is consistent with the existence of critical or supercritical upstream flow, which blocks mechanical information generated in the upstream basin from reaching the sill. The relevance of  $g'$  is consistent with the fact that density is advected by the flow and information about the density difference  $\Delta\rho$  can pass right through the control section. The value of  $g'$  has been regarded fixed throughout this discussion, but one would wish to eventually relax this constraint by allowing  $\Delta\rho$  to vary, say, in response to changes in forcing and/or mixing in the upstream basin. This topic will be pursued in Sections 5.5 and 5.6.

If the sill elevation  $h_m^*$  is decreased to zero, so that  $D_s / z_T^* = 1$ , the upstream and sill controls merge. The coalescence point *lies* at  $o$  (5.3.1b) where the critical diagonal makes grazing contact with the curve  $d_{1\infty} = 1.25$ . It can be shown (see Exercise 2) that both  $c_+$  and  $c_-$  are zero in this solution, which will emerge as an important type of flow through a contraction. It is left as an exercise to show that corresponding lower layer transport is given by

$$|Q_2^*| = (1 + |Q_r|^{1/2})^{-2} g'^{1/2} w^* D_s^{3/2}, \quad (5.3.4)$$

where  $D_s$  is now just the depth in the uniform channel. Larger values of  $|Q_2|$  correspond to (supercritical) solution curves lying entirely above the critical diagonal. These solutions do not connect directly to any geophysically relevant reservoir state, nor is it possible to connect the solutions to subcritical flow by hydraulic jumps along curves of constant  $q_2$ . Therefore (5.3.4) gives an upper bound on  $|Q_2|$  for relevant flow (i.e. flows that become subcritical somewhere upstream).

*e. Other constraints.*

In most cases of geophysical or engineering interest, geometrical variables like  $w^*$ ,  $h_m^*$ , and  $z_T^*$  are known in advance and  $d_{1\infty}^*$  can be estimated from hydrographic data. In addition, a relation between  $Q_1^*$  and  $Q_2^*$  can often be stipulated, such as when the strait connects with a closed basin with known evaporation  $E$  and precipitation  $P$ . (The flow rates are then constrained by  $Q_1^* - Q_2^* = \iint_{A_s} (E - P) dA$ , where  $A_s$  is the surface area of the basin.) These constraints are still insufficient to determine the parameters  $d_{1\infty}$ ,  $q_2$ , and  $Q_r$  required to fix the solution and the individual values of  $Q_1^*$

and  $Q_2^*$ . To do so, one must assume that the solution is critical at the sill, and perhaps in the approach, and use these conditions to close the problem.

As an example, consider the case where the upstream basin is infinitely deep and it is suspected that an approach (or exit) control *and* a sill control occur ( $d_{1\infty}=1.5$ ). For exchange flow, this would mean that the exchange transport is maximal. Further assume that the downstream basin is closed and has  $\iint_{A_s} (E - P)dA = 0$ , so that  $Q_r = -1$ . We have already shown that  $Q_2^* = -Q_1^* = .208 g'^{1/2} w^* D_s^{3/2}$  under these conditions. If  $|Q_r| \neq 1$ , then a more general version of the last relation can be used (see Exercise 3). If only a sill control exists, the flux is less constrained and it becomes necessary to measure the upstream interface level in order to close the problem.

*f. Experiments on two-layer sill flows.*

Laboratory and numerical experiments have proven valuable in determining whether the flows discussed above are realizable and in demonstrating how they can be established. By no means has all of the theoretically possible steady behavior been investigated. We discuss two revealing experiments, the first dealing with unidirectional flows and the second with exchange flows. A review of the work on unidirectional flows will help illustrate some of the differences with the exchange flows discussed above. The experiments were originally performed by Long (1954, 1970) who towed an obstacle through a two-fluid system initially in a state of rest. Extensions have been carried out by Houghton and Isaacson (1970), Baines (1984, 1987), and others. One setting for numerical computation of the flow has two layers initially moving from left to right with equal velocity and in a uniform channel ( $h^*=0$ ). Consider the case where this initial flow is subcritical and where the lower layer is much thinner than the upper layer. At  $t^*=0$  an obstacle of height  $h_m^*$  is placed in the path of the flow. Since the upper layer is relatively deep, the adjustment for moderate  $h_m^*/z_T^*$  is similar to that for a single-layer flow. If  $h_m^*/z_T^* \ll 1$ , the flow remains subcritical and there is no upstream influence. As  $h_m^*/z_T^*$  is increased, a critical value will be reached above which upstream influence occurs. The critical value is that required to establish critical flow over the sill for the upstream conditions given by the initial flow. The steady solution that develops over the obstacle will resemble solution *bcd* (Figure 5.3.1b) qualitatively. A slight increase in  $h_m^*/z_T^*$  past the critical value will result in the excitation of a bore that permanently alters the upstream flow by deepening the lower layer and decreasing the lower layer transport. Further incremental increases in  $h_m^*/z_T^*$  will have a similar effect. As long as the upper layer remains relatively inactive during this process, the linear wave speed ( $c_* \cong v_2^* - (g'd_2^*)^{1/2} < 0$ ) of the upstream flow increases in magnitude. As the obstacle height increases, it is possible for the lower layer to become completely blocked as a result of this process and further increases in  $h_m^*/z_T^*$  will cause the obstacle to protrude into the

upper layer. In this case, additional upstream changes are prevented.<sup>3</sup> Up to this point the evolution is similar to that found in the single-layer version of Long's experiment (Section 1.6).

If the lower layer remains unblocked, increases in  $h_m^*/z_1^*$  eventually lead to effects that are special to two-layer systems. To understand these changes, one should recall that growth of the obstacle does not alter the total volume transport  $Q_1^*+Q_2^*$ . Thus, the decrease in  $Q_2^*$  is compensated by an increase in  $Q_1^*$ . In addition, the upstream thickening of the lower layer results in a thinning of the upper layer. Both effects tend to bring the initially inactive upper layer into play upstream of the obstacle and a consequence is that the growth in  $-c^*$  is reversed. When the maximum value is reached, the bore achieves its maximum possible amplitude. As  $h_m^*/z_1^*$  increases  $c^*$  reaches a maximum negative value then moves towards positive values. The bore achieves its maximum amplitude where  $-c^*$  is maximum; the upstream disturbance beyond this threshold consists of a bore followed by a rarefaction. At some  $h_m^*/z_1^*$  this trend causes  $c^*$  to be reduced to zero: the upstream flow becomes critical. The flow over the obstacle now resembles the solution  $klmn$  of Figure 5.3.1b, qualitatively, with an upstream control and a sill control. The upstream critical section is called an *approach control*.

Although the shape of the interface and the distribution of layer Froude numbers in configuration  $klmn$  are the same as for the previously considered maximal exchange solution, there are some important differences. For one thing, the fact that the total volume transport remains fixed at its initial value makes it less meaningful to talk about maximal flux. (Maximal *exchange* on the other hand can be defined even when  $Q_1^*+Q_2^*$  is constrained to be zero.) Another difference can be seen by imagining, as we did earlier, that the channel broadens at some upstream location. The flow therein becomes supercritical, as before, but now the direction of wave speed propagation is *towards* the sill. If one follows this supercritical flow as it leaves the broad basin and enters the narrower portion of channel, the supercritical flow becomes critical and then subcritical. This arrangement focuses wave energy towards the approach control section and therefore gives rise to a shock forming instability.

Once the solution  $klmn$  is established, a slight increase  $h_m^*/z_1^*$  leads to interesting changes in the flow that may not be completely describable by hydrostatic theory. In order to understand these changes, it is helpful to remember that the upstream propagation speed has already been reduced to zero by the rarefaction triggered by previous adjustment. A new rarefaction caused by a further increase in  $h_m^*/z_1^*$  would therefore be unable to propagate upstream. Numerical simulations with hydrostatic models have shown, in fact, that such an increase causes the flow over the obstacle to revert to a supercritical, symmetrical state, while the approach control is maintained. The flow near the obstacle now resembles solution  $kjk$ , with an approach control but no sill control. Beyond this point, increases in  $h_m^*/z_1^*$  lead to no further upstream influence. Laboratory experiments give a somewhat different picture for the flow downstream of the

---

<sup>3</sup> Additional increases in the obstacle height will only impede the upper layer flow if frictional or non-hydrostatic effects come into play.

sill. Here a nonhydrostatic, and possibly dissipative, feature known as a *supercritical leap* may form (Lawrence, 1993 and Zhu and Lawrence, 1998). The ‘leap’ is a smooth transition from one supercritical state with a deep lower layer to another supercritical state with a shallower lower layer. This transition occurs on the downstream face of the obstacle and can be followed by a hydraulic jump.

The initial value problem has also been investigated for cases in which the initial lower layer depth is not small. The sequence of events that takes place may be different from what is described above and the reader is referred to Baines (1995, Chapter 3) for a thorough discussion. A fundamental point to keep in mind is that the formation of the upstream control, the central departure from single-layer hydraulics, occurs because  $-c_*$  has a maximum value in the upstream flow at an intermediate interface level.

Turning now to the case of exchange flow, we review an experiment (Zhu and Lawrence, 2000) that shows how maximal and submaximal states can be established. As shown in Figures 5.3.2(a,b), the channel contains an isolated obstacle and opens abruptly at either end into wide reservoirs. The right and left reservoirs are initially filled to the top with fluids of slightly different densities, the left reservoir containing the denser fluid. A barrier that sits atop a sill separates the two fluids. The barrier is removed and the two fluids are allowed to displace each other. After an initial period of transient activity, the flow within the channel settles into a nearly steady state. The layer velocities in the left reservoir are relatively weak and the upper layer depth therefore approximates  $d_{1\infty}^*$ . Initially, this depth is relatively small (Figure 5.3.2c), but it gradually increases as lower layer fluid is drained out of the reservoir. An exit control occurs near the left end of the channel (point  $k$ ) and the flow immediately to the right is subcritical. To the left there is a brief span of supercritical flow. Ideally, this flow would be joined to the reservoir flow by a hydraulic jump. In the experiment, the supercritical flow actually enters the reservoir as a concentrated jet that gradually disperses. The flow near the jump is horizontally two dimensional due to the abrupt widening of the geometry. At the sill the subcritical flow passes through a second control and becomes supercritical. A hydraulic jump occurs on the right slope of the obstacle and the flow thereafter is subcritical. From the left end of the channel to the hydraulic jump the interface resembles the solution  $klmn$  of Figure 5.3.1b. The transition from the left end of the channel into the left reservoir cannot be traced in this figure but is discussed below. While in this configuration,  $|Q_1^* - Q_2^*|$  remains fixed at its maximal value, the determination of which is described in Exercise 4.

As the left reservoir loses lower-layer fluid, the interface there falls and the hydraulic jump moves closer to the entrance (point  $k$ ) of the channel. At the same time, conditions in the channel between the exit control and the sill control remain steady; the supercritical end states insulate that part of the flow from the two reservoirs. However, the interface in the left reservoir eventually becomes low enough that the hydraulic jump reaches the position of the exit control. The exit control becomes ‘flooded’, the flow there becomes subcritical, and the exchange becomes submaximal and dependent on the upstream interface elevation. This elevation continues to decrease and the exchange flux with it.

## Exercises

- 1) For arbitrary  $Q_r$ , which constant energy curve makes grazing contact with the critical diagonal in Figure 5.3.1a?
- 2) For the solution designated by the point  $o$  in Figure 5.3.1b, prove that under conditions of pure exchange flow,  $c_+^* = c_-^* = 0$ .
- 3) Consider the case of flow over an obstacle with the lower layer originating from an infinitely deep basin. If the flow has an exit control and a sill control, show that  $d_{1\infty} = 1.5$  regardless of the value of  $Q_r$ . Further show that the transport in the lower layer is given the generalized weir formula:

$$Q_2^* = [Q_r^{2/3} F_{1c}^{-2/3} + (1 - F_{1c}^2)^{-1/3}]^{-3/2} g'^{1/2} w^* D_s^{3/2}$$

where  $F_{1c}$  is determined from

$$F_{1c}^{4/3} - Q_r^{-2/3} (1 - F_{1c}^2)^{2/3} + 2F_{1c}^{-2/3} = 3.$$

- 4) In the experiment of Zhu and Lawrence (2000), described in part *c*, a maximal exchange flow was observed. The values of  $w^*$ ,  $g'$ ,  $z_1^*$ , and  $h_m^*$  are set by the geometry and by the initial conditions and it is also known, due to the closed geometry of the channel and reservoir system, that  $Q_r = -1$ . To predict the maximal value of  $Q_2^*$ :

(a) Show that

$$F_{1e}^{4/3} - (1 - F_{1e}^2)^{2/3} + 2F_{1e}^{-2/3} = F_{1s}^{4/3} - (1 - F_{1s}^2)^{2/3} + 2F_{1s}^{-2/3},$$

where the subscripts  $e$  and  $s$  correspond to exit and sill. (Hint: use energy conservation between the exit and sill along with the critical condition at both locations.)

(b) Further show using volume flow rate continuity that

$$\begin{aligned} Q_2 &= g'^{1/2} w^* (z_T^* - h_m^*)^{3/2} [F_{1s}^{-2/3} + (1 - F_{1s}^2)^{-1/3}]^{-3/2} \\ &= g'^{1/2} w^* (z_T^*)^{3/2} [F_{1e}^{-2/3} + (1 - F_{1e}^2)^{-1/3}]^{-3/2} \end{aligned}$$

This gives three equations for the unknowns  $F_{1e}^2$ ,  $F_{1s}^2$ , and  $Q_2$  in terms of the known  $w^*$ ,  $z_1^*$ , etc.

5) Calculation of the coefficient  $q_2(D_s / z_T^*)$  in equation 5.3.3. Consider a solution for flow in a channel with constant width and with  $|Q_r|=1$ . The flow has two control points corresponding, say, to points  $k$  and  $m$  in Figure 5.3.1b. Show that the values of the lower layer Froude numbers at  $k$  and  $m$  can be computed from the relations:

$$\frac{Q_r^{2/3} F_{1m}^{-2/3} + (1 - F_{1m}^2)^{-1/3}}{Q_r^{2/3} F_{1k}^{-2/3} + (1 - F_{1k}^2)^{-1/3}} = \frac{D_s}{z_T^*}$$

and

$$\frac{1}{2} F_{1m}^{4/3} - \frac{1}{2} Q_r^{-2/3} (1 - F_{1m}^2)^{2/3} + F_{1m}^{-2/3} = \frac{1}{2} F_{1k}^{4/3} - \frac{1}{2} Q_r^{-2/3} (1 - F_{1k}^2)^{2/3} + F_{1k}^{-2/3}.$$

Here  $z_T^*$  is the total depth upstream of the obstacle (where  $h^*=0$ ). Once  $F_{1m}$  has been calculated from these relations,  $F_{2m}$  follows from the critical condition  $G^2=1$ . Then  $q_2$  follows from (5.3.2).

6) For the maximal solution with a deep upstream basin and with  $|Q_r|=1$ , show that  $d_{1\infty}^*$  is 0.53 times the depth over the sill. That is, the interface in the hypothetical wide upstream basin lies about half the sill depth.

7) Prove the result 5.3.4.

## Figure Captions

Figure 5.3.1 (a) The Froude number plane showing solution curves for flow over a variable bottom in a channel with constant width and  $|Q_r|=1$ . Contours of constant internal energy  $d_{1\infty}$  are represented by thick lines. Continuous solutions must lie along these contours. The thin contours represent constant  $q_2$ . For a fixed layer flux  $Q_2^*$ , larger values of the topographic height  $h^*$  correspond to smaller  $q_2$ . (From Armi, 1986)

Figure 5.3.1 (b) A portion of the Froude number plane in (a) with examples of various solutions sketched in the insets.

Figure 5.3.2 The experimental setup used by Zhu and Lawrence (2000) to simulate a lock exchange.

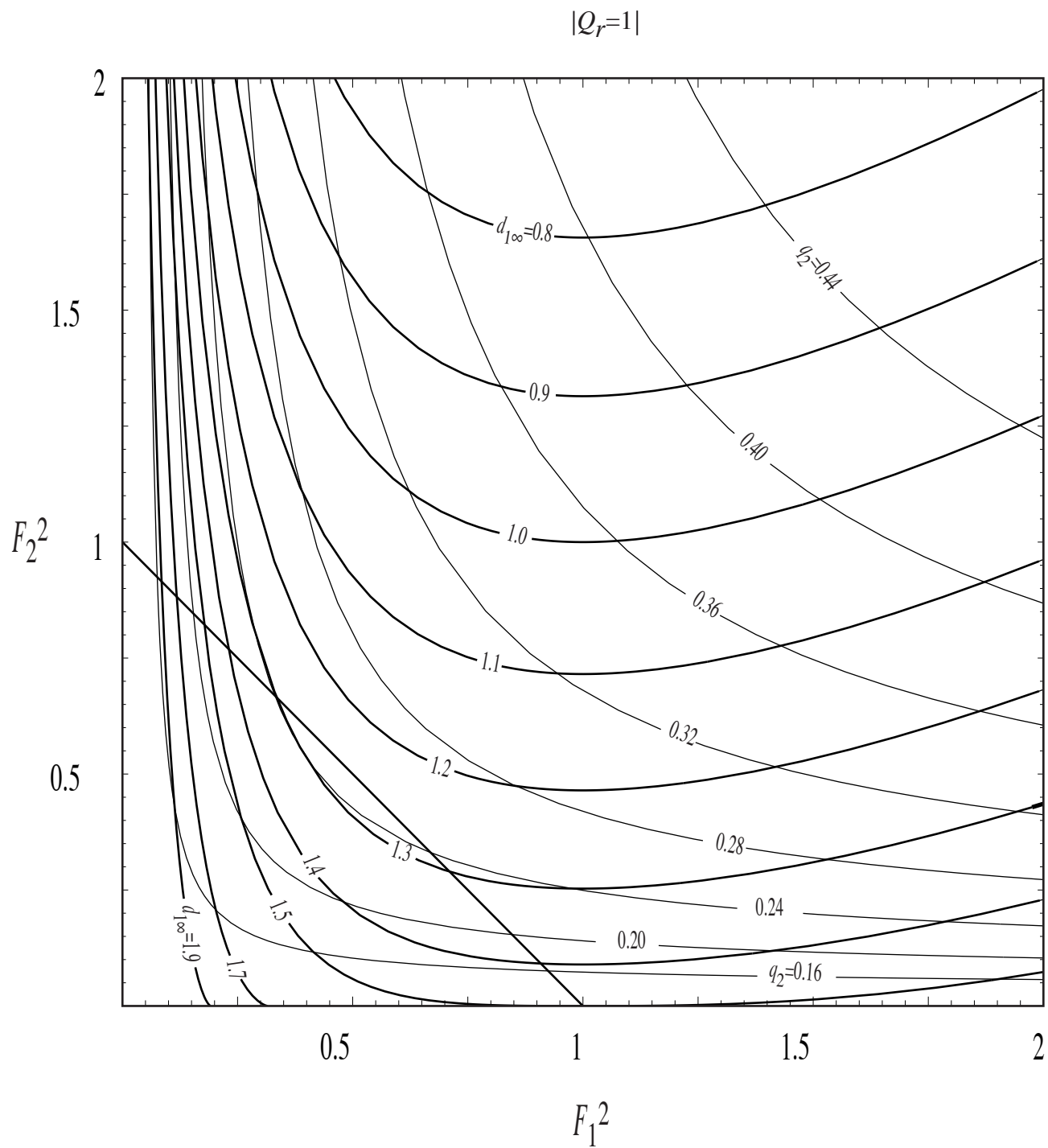


Figure 5.3.1a

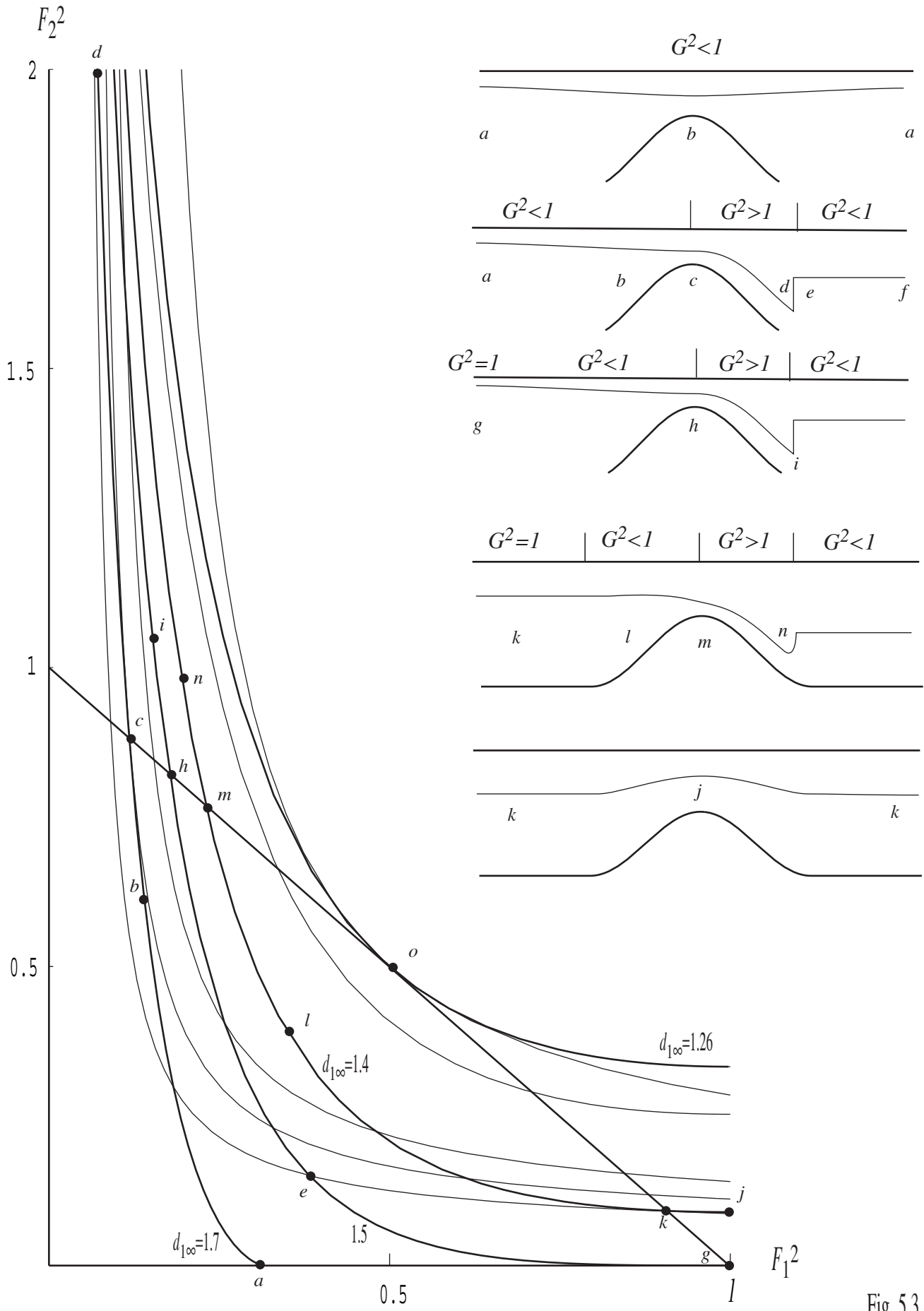


Fig. 5.3.1b

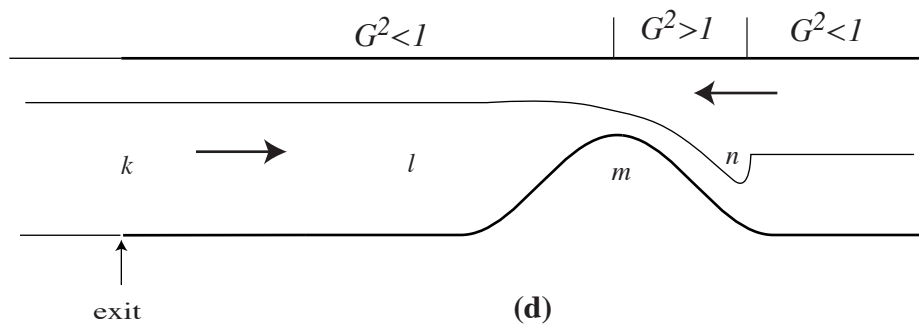
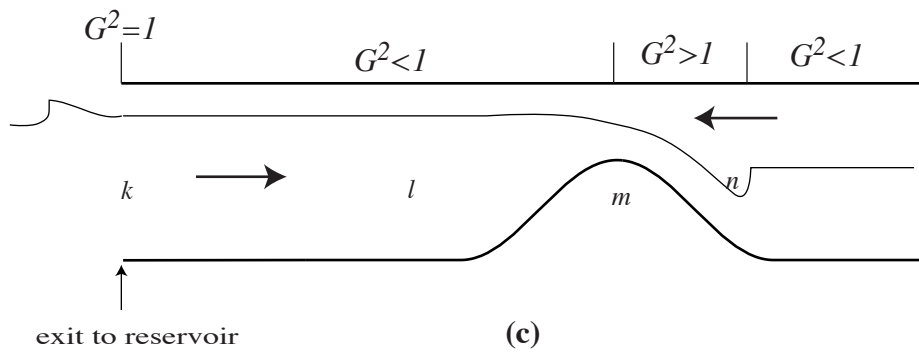
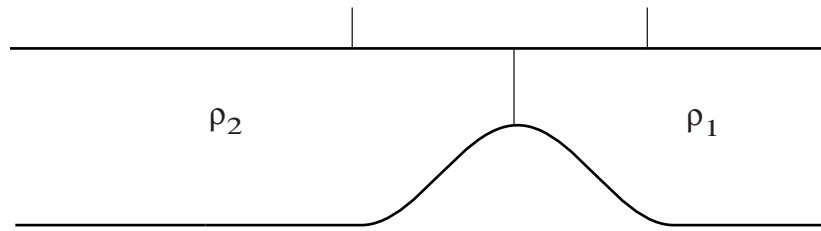
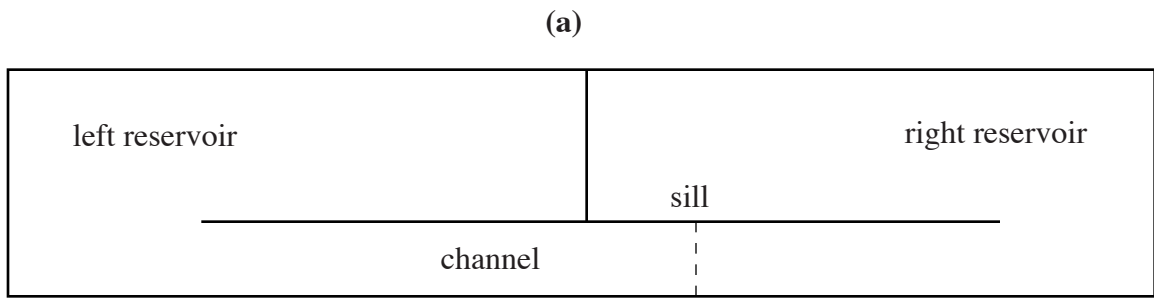


Fig. 5.3.2